Zeitschrift für Physikalische Chemie, Bd. 208, S. 77–91 (1999)

Effect of Chloride Anions on Cu Electrodeposition onto Pt(110) and Pd(110) Surfaces*

By M. S. Zei

Fritz-Haber Institut der Max-Planck-Gesellschaft,
Faradayweg 4–6, D-14195 Berlin, Germany

(Received October 29, 1997; accepted December 4, 1997)

Adsorption / Electrochemistry / Electron diffraction / Electrochemistry of solids / Epitaxy

Cyclic voltammetry for Cu UPD on Pd(110) in H_2SO_4, $HClO_4$ and in Cl^- containing solutions has been studied in comparion with Cu UPD on a Pt(110) surface. The structural properties of Pd(110) and Pt(110) after Cu UPD in different electrolyte solutions were investigated by LEED, RHEED and Auger electron spectroscopy. Structural models for Pd(110) covered by 1 and 2 ML Cu, derived from the coulometric charge, AES measurements and the diffraction data are presented.

Specific adsorption of SO_4^{2-}/HSO_4^- anions causes the formation of ordered $c(2\times4)$ and $c(2\times2)$ structures on Pt(110) and Pd(110) respectively. In the presence of chloride ions, specific adsorption of Cl on the Cu/Pd(110) surface gives rise to a pronounced change in the voltammogram and results in two ordered superstructures, while on Pt(110) no specific adsorption of Cl takes place.

1. Introduction

The underpotential deposition of Cu on a Au(111) surface has been extensively studied [1–4]. Cyclic voltammetry for Cu UPD onto Au(111) showed the deposition in two distinct adsorption states [3, 5] which has been previously investigated by *ex situ* LEED/RHEED studies [3]: In the first stage, correponding to the more positive Cu deposition peak (2/3 ML Cu coverage), the Cu adatoms form a $(\sqrt{3}\times\sqrt{3})R30°$ superstructure and in the second stage it forms a commensurate (1×1) monolayer after 1 ML Cu deposition which has been confirmed by both *in situ* STM [6, 7] and *in situ*

* Presented at the *5. Ulmer Elektrochemische Tage* on "Fundamental Aspects of Electrolytic Metal Deposition", June 23–24, 1997.

EXAFS studies [8]. In the past Cu on Pt(111) was not studied as extensively as Cu on Au(111). The cyclic voltammetry for Cu UPD on Pt(111) only showed one pronounced peak corresponding to a commensurate Cu (1×1) monolayer on the Pt(111) surface [9, 10]. Recently, the Cu UPD onto Pt(111) in the presence of chloride ions has also been extensively studied [9–12]. The Cl^- ions had a dramatic effect on the UPD of Cu on Pt(111), giving rise to two very sharp voltammetric features. The Cl adlayer structure deduced from the *ex situ* LEED observations [9, 10] is in agreement with those obtained by *in situ* STM [13] and X-ray scattering measurements [11], even though there is some controversy as to the determination of Cu coverage at the potential between the two voltammetric peaks. These results demonstrate that the emersion process does not disrupt the adlayer structures on the electrode surface of Au(111) [3, 6] and Pt(111) [7, 9, 13].

The Pd(110) surface is of importance for electrocatalysis. To our knowledge, unfortunately, there is no report for Cu electrodeposition on a well-characterized Pd(110) surface. This may be due to the problems related to the preparation and handling of the clean electrode surface in an electrochemical environment. So it is interesting to investigate the structural properties of Pd(110) after Cu deposition as well as the voltammogram in comparison with the results reported recently for Cu UPD on Pt(110) [14, 16].

In the following we present the results of Cu UPD on Pd(110) in comparison with the Cu deposition on Pt(110) in sulfuric and in Cl^- containing solutions. The Pd(110) and Pt(110) electrode surfaces were prepared in UHV and the surface structure investigated by *ex situ* LEED/RHEED before and after the electrochemical experiments. The Cu underpotential deposition on Pd(110) also showed two distinct stages similar to that observed for Cu UPD on Pt(110) and Au(111). A structural model is proposed based on the coulometric charge, AES measurements and diffraction data.

2. Experimental

The experimental set-up, including a UHV system with LEED, RHEED (Reflection High Energy Electron Diffraction) and AES, electrochemical cell and a closed sample transfer, has been described previously [17]. The electrode, a single crystal disc of 8 mm diameter and 2 mm thickness, was mounted between tungsten wires which also served for resistive heating of the sample. The electrode surface was prepared by cycles of sputtering (Ar^+, 30 min, 5×10^{-5} mbar, 600 °C), until AES and LEED/RHEED indicated the formation of clean and ordered surfaces. This treatment was repeated after each electrochemical experiment. The electrolyte solutions, 0.01 M H_2SO_4, 1 mM $CuSO_4$, 0.01 M $HClO_4$ and HCl (E. Merck, suprapur) were made with triply distilled water. All potentials are referred to a Ag/AgCl reference electrode.

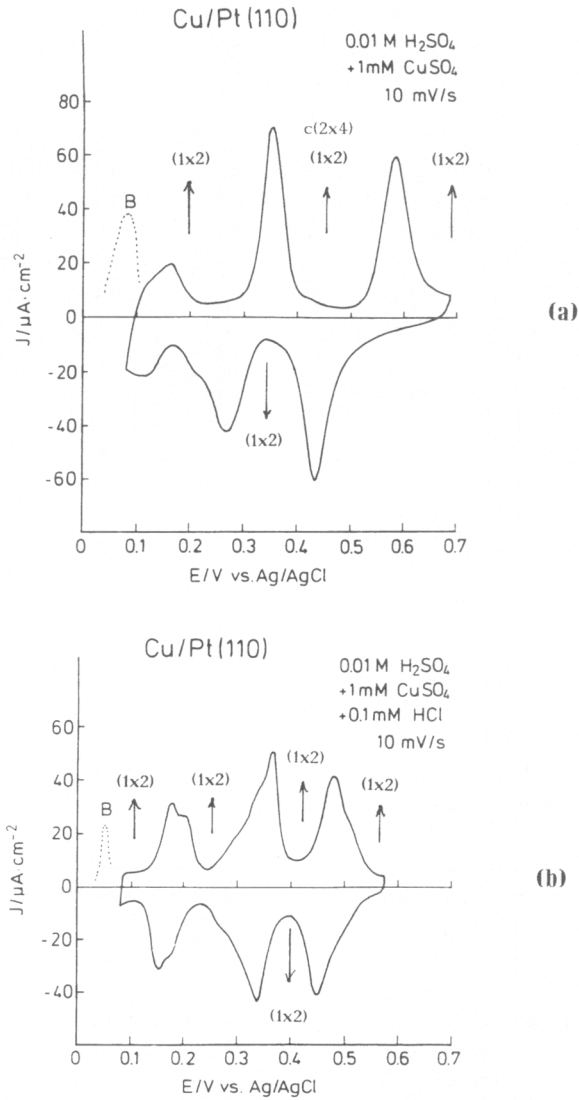

Fig. 1. Cyclic current-potential curves for the underpotential deposition (UPD) of Cu on Pt(110) electrode. a) in 0.01 M H_2SO_4 + 1 mM $CuSO_4$, scan rate 10 mV/s. b) in 0.01 M H_2SO_4 + 1 mM $CuSO_4$ + 0.1 mM HCl.

3. Results and discussion

Copper adsorption on Pt(110)-(1×2)

The cyclic voltammogram for Cu UPD on Pt(110)-(1×2) in sulfuric acid solution (Fig. 1a) clearly shows that the full coverage of Cu on Pt surface

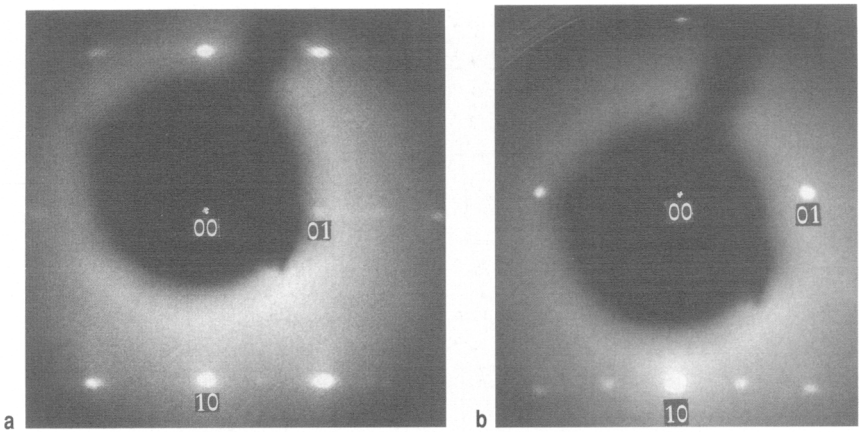

Fig. 2. LEED patterns for Pt(110) electrode emersed from 0.01 M H_2SO_4 + 1 mM $CuSO_4$ + 0.1 mM HCl solution a) at +0.4 V between two dissolution peaks, showing weaker intensity for the half-order reflection (72 eV). b) at +0.2 V, showing a (1×2) structure with nearly equal spot intensity for (0,1) and (0,1/2) beams (52 eV).

is formed in two energetically well-separated steps which is similar to previous reports by Kolb *et al.* [14] and Aberdam *et al.* [15], who also observed two voltammetric peaks. From the coulometric charge and the Auger measurements for the Cu deposit, it was concluded that each current peak is associated with 1 ML Cu coverage on the reconstructed Pt(110) surface. This is also supported by the structure analysis [16]: the expected LEED patterns are in good agreement with the experimentally observed LEED patterns which are identical to those obtained in Cl containing solution as shown in Fig. 2. It reveals no spot-broadening neither in ⟨110⟩ nor in ⟨100⟩ directions, suggesting that the Cu adatoms are sitting at preferred adsites along the ⟨110⟩ troughs and that the coherent 2**a** spaced rows of Cu adatoms are not randomly distributed along ⟨110⟩ troughs (**a** is the Pt lattice constant). The resulting structure would be identical to that of a (1×2) surface, except for every trough of the surface Pt atoms being covered by 2 rows of Cu atoms. Also no spot-broadening of the integer-order beams for the Pt(110) electrode emersion at +0.2 V has been observed where the electrode was completely covered by Cu adatoms (2 ML). A drawing of the proposed structure for these diffraction patterns is shown in a previous paper [16]. If the 2**a** spaced rows of Cu adatoms are randomly shifted in the ⟨110⟩ direction, a diffuse streak perpendicular to the ⟨110⟩ direction should be observed at (0,1/2) spot. It has been confirmed by the investigations for Na adsorption on Ni(110) with a (3×3) structure: the triple-spaced rows of Na adatoms are randomly shifted in the ⟨110⟩ direction on Ni(110), producing a streak at (0,1/3) diffraction spot in the ⟨001⟩ direction [18].

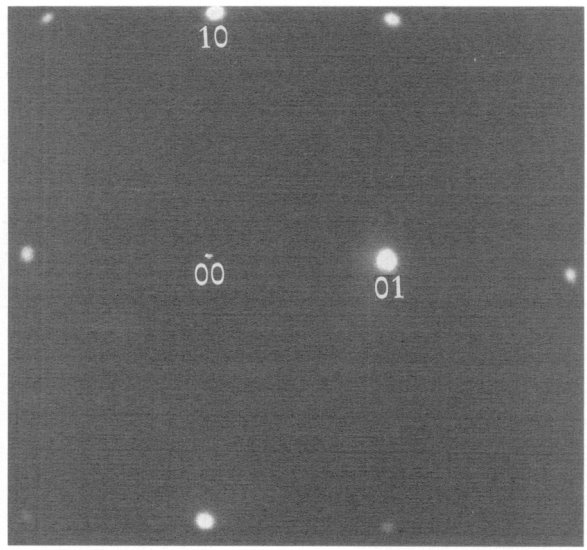

Fig. 3. (1×1) LEED pattern (61 eV) from the Pd(110) surface after preparation by sputtering and annealing in the UHV chamber.

In the presence of Cl ions, the voltammetric peaks became broader and the stripping peak at more positive potential shifted 120 mV negatively, while the stripping peak at more negative potential and the charge associated with each current peak remained unchanged as shown in Fig. 1b. The (1×2) structure (Fig. 2) was observed after electrode emersion at potentials indicated by the arrows in Fig. 1b, showing that the reconstruction is stable against chloride anion adsorption and Cu deposition since after stripping and emersion at +0.6 V the Pt electrode still revealed a (1×2) structure in agreement with the LEED investigations by Kolb *et al.* [14]. These results are surprising: The reconstructed Pt(110) surface is not only stable against hydrogen, sulfate [14] and chloride adsorption but also against Cu deposition. This is in contrast to the reconstructed Au(110) surface which has been shown to be stable only in perchlorate solution [14], while sulfate, or chloride adsorption [19] or small amount of Cu deposit removes the (1×2) reconstruction [20].

Copper adsorption on Pd(110)

The clean Pd(110) surface shows a (1×1) structure (Fig. 3), indicating that the topmost Pd(110) layer is not reconstructed after the cleaning process. The cyclic voltammetry for Cu UPD on Pd(110) electrodes in sulfuric acid and in perchlorate solutions are almost identical (see Figs. 4a and 4b), also

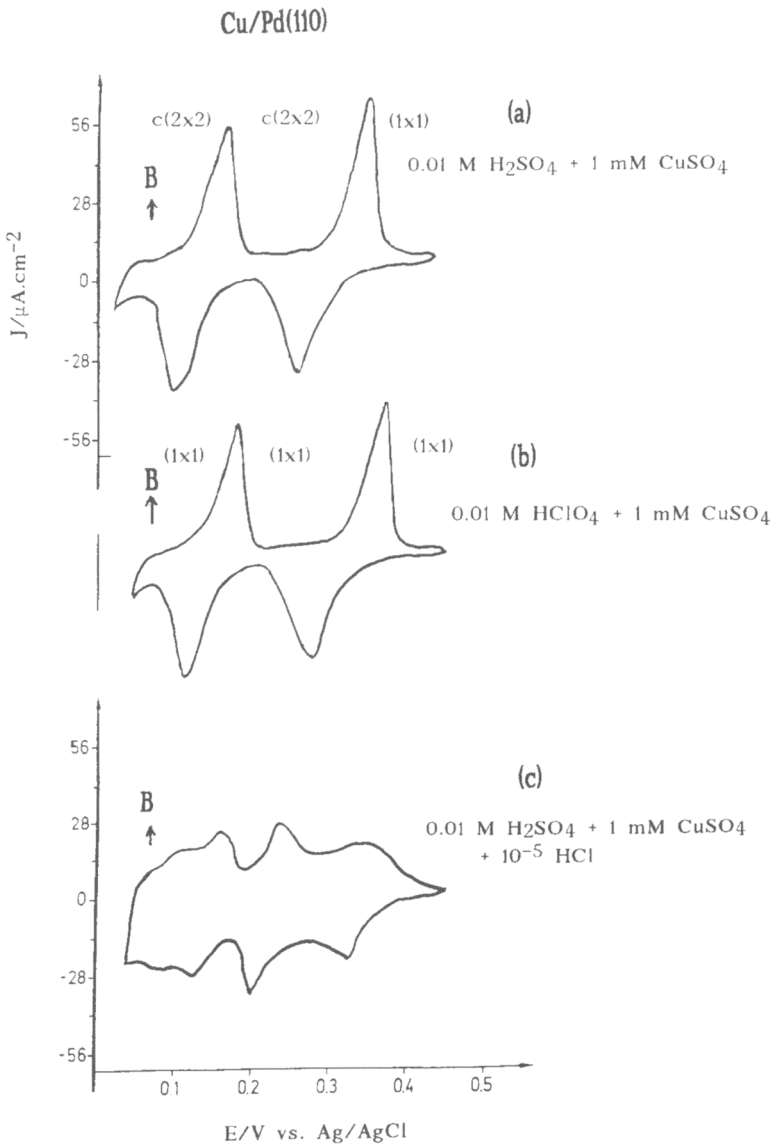

Fig. 4. Cyclic current-potential curves for Cu UPD on Pd(110) electrode. a) in 0.01 M H_2SO_4 + 1 mM $CuSO_4$. b) in 0.01 M $HClO_4$ + 1 mM $CuSO_4$. c) in 0.01 M H_2SO_4 + 1 mM $CuSO_4$ + 10^{-5} M HCl. Scan rate 10 mV/s.

showing two well-separated Cu UPD peaks similar to those observed for Cu UPD on Pt(110) (Fig. 1). The coulometric charge for each current peak is close to 300 μC/cm² corresponding to 1 monolayer of Cu coverage. This

Table 1. Comparison of AES peak ratios and corresponding Cu coverages with the coulometric data.

System	Emersion potential	Q ($\mu C/cm^2$)	Θ (ML)	I_{Cu}/I_{Pd}	Θ^{AES} (ML)	Electrolyte
Cu/Pt(110)	+0.45 V	300	1			1 mM $CuSO_4$
	+0.2 V	600	2			+0.01 M H_2SO_4
Cu/Pd(110)	+0.3 V	295	1	0.46	0.9	+0.01 M $HClO_4$
	+0.1 V	585	1.95	0.86	1.9	
	+0.28 V	285	0.96	0.5	1	+0.01 M H_2SO_4
	+0.15 V	572	1.91	1.0	2.3	
Cu/Pd(110)	+0.21 V	–		0.45	0.9	+0.01 M H_2SO_4
	+0.11	–		1	2.3	$+10^{-5}$ M HCl
Cu/Pd(100)	+0.18 V	355	0.83–0.9	0.6	1	+0.01 M H_2SO_4

conclusion is in agreement with the AES estimation for Cu deposit which was derived by the Auger peak ratio I_{Cu}/I_{Pd} calibrating with 1 ML Cu deposited on Pd(100) surface (see Table 1). The Cu bulk deposition takes place at 0.025 V (Nernst reversible potential) as indicated by B in Fig. 4, where the Cu thickness is in $t^{1/2}$ manner to the deposition time. LEED patterns show a c(2×2) structure for the Pd(110) electrodes emersed at +0.1 and +0.3 V where the Pd electrode was covered by 2 and 1 ML Cu respectively. The adsorption of sulfate ions causes a c(2×2) superstructure to form, while the Cu adatoms form a pseudomorphic adlayer on Pd(110) which will be discussed below.

The LEED pattern (Fig. 5a) from Pd(110) shows a (1×1) periodicity after deposition of 1 ML Cu in perchlorate solution, in which the electrode was emersed at +0.3 V between the two current peaks. Except for diffuse background due to the electrolyte adsorbate, there is no discernible spot-broadening in the LEED pattern which suggests that one-dimensional parallel Cu rows are not randomly distributed and are composed by atoms periodically spaced by a distance of 2.75 Å along the ⟨110⟩ troughs, being commensurate with the Pd substrate surface. The **a** spaced ⟨110⟩ rows of Cu adatoms cover regularly a flat Pd(110) surface as demonstrated by the reflection streaks in RHEED pattern (Fig. 5a). A structural model for one monolayer Cu coverage on Pd(110)-(1×1) electrode is shown in Fig. 6a which was derived from the charge, AES measurements for Cu deposit and the diffraction patterns. The resulting structure is identical to that of a bare

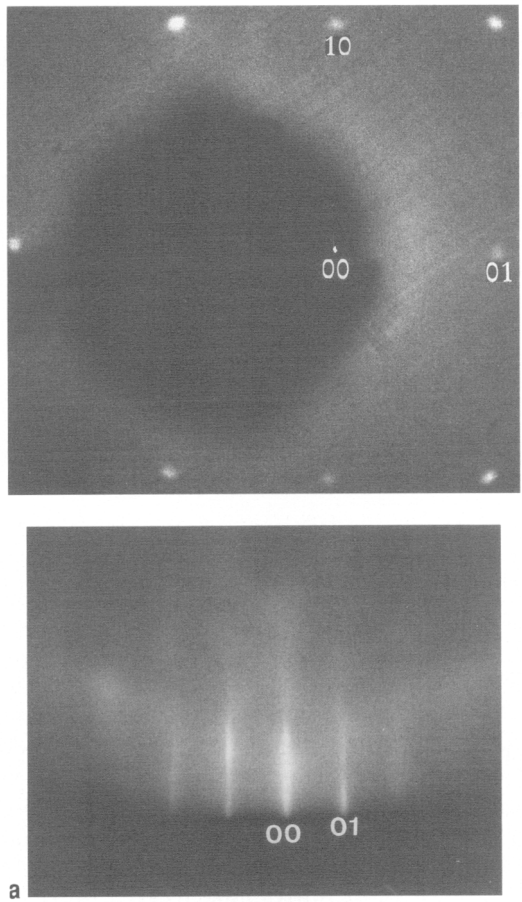

Fig. 5. LEED/RHEED ($\langle 110 \rangle$) patterns for Pd(110) electrodes emersed from 0.01 M $HClO_4$ + 1 mM $CuSO_4$ solution. a) at +0.26 V. b) at +0.11 *V*., showing a (1×1) structure.

(1×1) Pd surface, except for every trough of Pd along $\langle 110 \rangle$ direction being filled by a row of Cu atoms. After emersion at +0.1 V, LEED patterns from the Pd(110) electrode also show a sharp (1×1) structure (Fig. 5b), where the AES peak ratio Cu/Pd is about $0.9-1.0$ corresponding to 2 ML Cu. This may indicate that the second Cu monolayer is also formed by one-dimensional parallel rows which are coherently spaced by a distance equal to the Pd lattice constant. Thus the Cu adatoms form commensurate (1×1) rows on the Pd substrate in the $\langle 110 \rangle$ direction. The electrode surface is now completely covered by Cu adatoms resulting in no Pd atoms being exposed to the electrolyte. The proposed structural model is shown in Fig. 6b. The

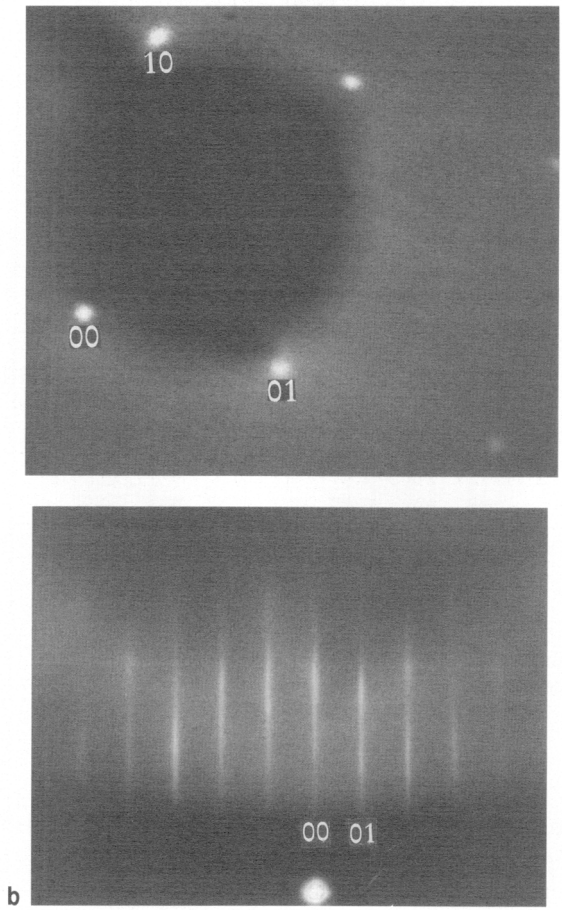

Fig. 5 (continued).

same is true for the case of Cu deposition onto Pd(110) in sulfuric acid solution, except for an additional superstructure c(2×2) due to sulfate ions on the Cu overlayer. The underpotential deposition of Cu on Pd(110) and Pt(110) shows that the complete Cu coverage consists of two distinct stages like in the case of Cu UPD on Au(111). However, the charge associated with the current peaks differs from that obtained from CuUPD on Au(111), where the Cu coverage of the first stage was 2/3 ML [5] and the charge ratio peak I/peak II was 2.

In the presence of Cl^-, a pronounced change in voltammetry for Cu UPD on Pd(110) can be seen in Fig. 4c, where two energetically well-separated current peaks, corresponding to the two Cu binding energies of

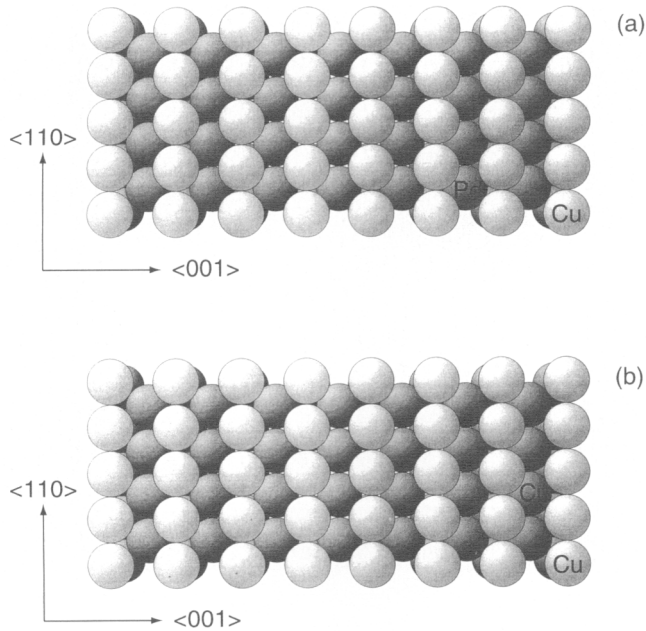

Fig. 6. Structure models (a) for 1 ML Cu deposited on the Pd(110)-(1 × 1) surface. b) for 2 ML Cu deposited on the Pd(110)-(1 × 1) surface.

3.71 and 4.09 eV, are no longer dissolved like that obtained from Cl^--free solution (Figs. 4a and 4b). Now, it shows several broad peaks overlapping each other, so a clear assignment of the voltammetric peak with respet to the binding energy and the Cu coverage is no longer possible as was done in the Cl^--free solution. This clearly indicates a very strong interaction between the Cu adatoms and the Cl coadsorbates on the Pd(110) surface. This is in contrast to the observation of the influence of Cl^- on the UPD of Cu on Pt(110) which shows only slight effects on the I-E curve (see Fig. 1b).

An interesting comparative feature between metal adsorption on single crystal surfaces under UHV conditions and electrodeposition on a single crystal surface is that the metal deposited overlayer generally requires heating to produce good ordering, while the electrodeposited Cu adlayer on Pt and Pd surfaces are already very well ordered at room temperature as demonstrated by the diffraction patterns for Cu on Pt(110) and Pd(110) as well as Cu UPD on Au(111) [3, 6, 7] and Pt(111) [9, 10]. This is obviously due to the influence of the anion coadsorption as has been confirmed by *in situ* EXAFS and X-ray scattering study for the adsorption of HSO_4^-/SO_4^{2-}

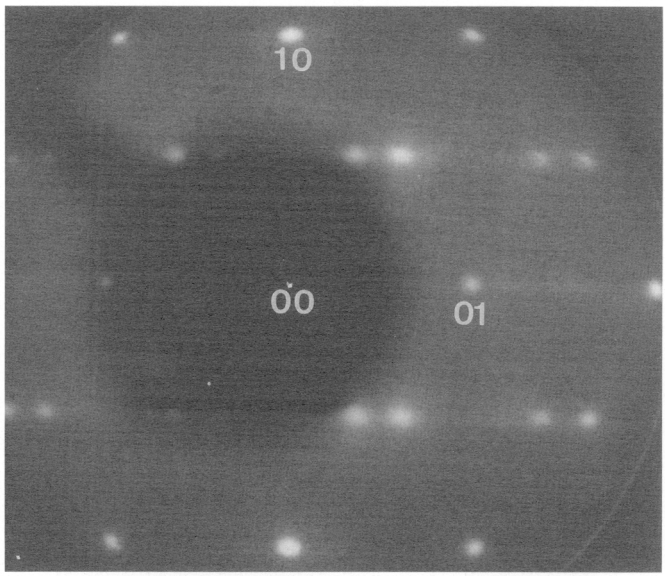

Fig. 7. c(2×2) LEED pattern (63 eV) for Pd(110) electrode emersed from 0.01 M H_2SO_4 + 1 mM $CuSO_4$ solution at +0.35 V i.e., between two dissolution peaks, showing a spot-splitting at (1/2,1/2).

on Cu/Au(111) [8] and Cl on Cu/Pt(111) [12] and *in situ* STM study for sulfate and chloride on Cu/Pt(111) [7, 13]. The adlayer seems to be stabilized by strong attractive interactions between copper and coadsorbate.

Superstructures formed by specific adsorption of anions on Pt(110) and Pd(110) after Cu deposition were analyzed. The LEED pattern of a Pt(110) electrode shows a c(2×4) superstructure after dissolution of the second ML Cu, when the electrode was emersed from the sulfuric acid solution at +0.45 V, i.e., between the two current peaks. The c(2×4) superstructure is no longer visible after rinsing with tri-distilled water. In other potential regions, it does not form this c(2×4) structure. In addition, in Cl^- containing solutions, this superstructure did not appear except for a (1×2) structure due to the reconstructed Pt(110) substrate. Hence we interpret the c(2×4) superstructure as an ordered adlayer of SO_4^{2-}/HSO_4^- anions on the Cu deposited Pt(110) surface. On the other hand, a c(2×2) superstructure was observed for Pd(110) after deposition of one or two ML of Cu in the sulfuric acid solution, while in the perchlorate solution it always showed a (1×1) structure. This may suggest that the c(2×2) superstructure is due to the adsorption of SO_4^{2-} anions on Cu covered Pd(110) surface. It is worth to note that Pt(110) and Pd(110) electrodes show a (1×2) and (1×1) structures, respectively after stripping and emersion at 0.5 V, where the elec-

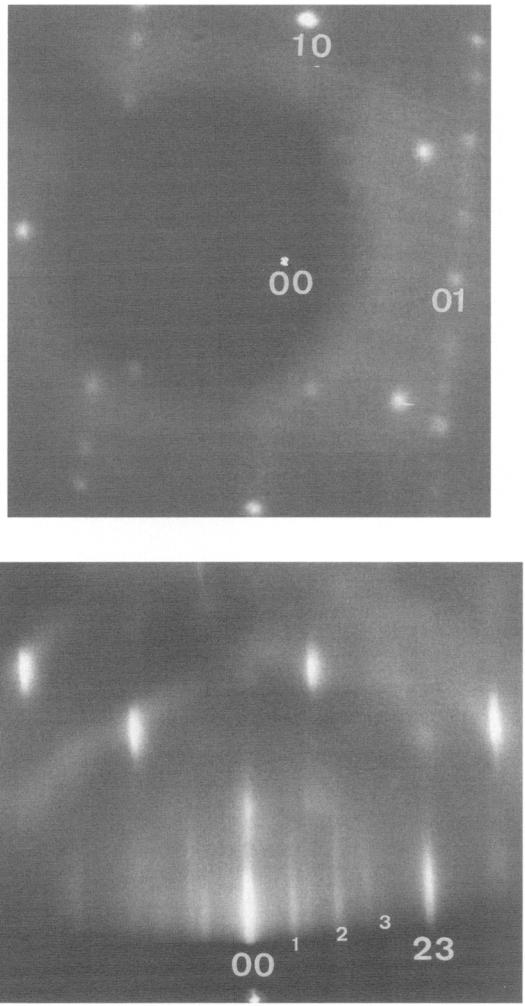

Fig. 8. (a) LEED (70 eV) and RHEED patterns from Pd(110) electrode emersed from 0.01 M H_2SO_4 + 1 mM $CuSO_4$ + 10 $^{-3}$ M HCl solution at +0.28 V, showing s1 and s2 superstructures. (b) structure models for the ordered $s1 = \begin{pmatrix} 1 & 0.41 \\ -1 & 0.59 \end{pmatrix}$ and $s2 = \begin{pmatrix} 1 & 2/3 \\ 1 & -2/3 \end{pmatrix}$ adlayers formed by Cl adatoms.

trodes were free from the copper deposit. This demonstrates that copper adsorption on Pt(110) and Pd(110) electrodes promotes coadsorption of sulfate anions, giving rise to ordered c(2×4) and c(2×2) structures, respectively. Further, a spot-splitting at (1/2,1/2) in the LEED pattern (Fig. 7)

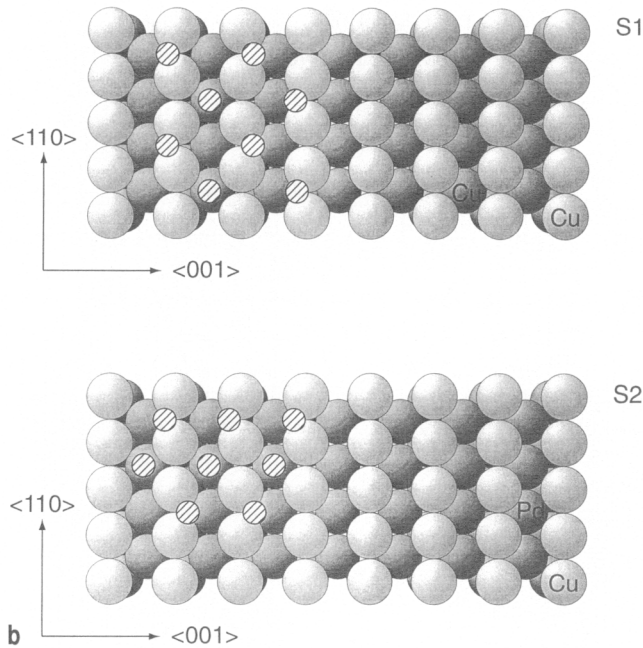

Fig. 8 (continued).

was observed from the Pd electrode emersed at 0.35V, i.e., between the two dissolution peaks, from the sulfuric acid solution. The spot-splitting in ⟨100⟩ direction can be explained by scattering of the antiphase domains of the c(2×2) adlayer [21] with a mean domain size of 16 Å estimated from the separation of the spots of the fractional-order beam [22, 23]. However, the integral-order spots (Fig. 7) remain sharp, indicating that the domain-separation (antiphase boundaries) must be integral multiples of the fundamental spacing. The formation of antiphase domains may be explained by the rearrangement of the c(2×2) adlayer after dissolution of the one monolayer Cu deposit: When the electrode potential was cathodically cycled to 0.1 V, the Pd electrode was covered by 2 ML Cu. After the potential was cycled up to 0.35 V, one monolayer of Cu deposit with some of sulfate coadsorbate was stripped from the Pd electrode. The LEED pattern for the Pd electrode emersed at 0.35 V shows a spot-splitting at (1/2,1/2). It is obvious that the remaining sulfate adsorbate rearranges again to form a c(2×2) on the partially Cu covered Pd electrode surface (50% Pd electrode is covered by Cu), leading to antiphase domains induced presumably by the surface defects [24].

In the presence of chloride ions, the LEED pattern from the Pd(110) electrode emersed at +0.19 V shows a s1 superstructure, while it shows s1

and s2 superstructures superimposed as shown in Fig. 8a for the electrode emersed at +0.3 V. The (h0) beams of s2- reciproal lattice can be clearly seen in the RHEED pattern and its 4th-order beam coincided exactly with the (23) substrate reflection. Thus the assignment of the 2D-reciprocal lattice of s2 by LEED is proven by the RHEED pattern (Fig. 8a). The structural models for s1 and s2 are presented in Fig. 8b. The s1 and s2 superstructures are attributed to the ordered Cl adlayer whose coverages (0.75–1 ML) are close to the value of 0.8–1.1 ML obtained from AES measurements for Cl (calibrated from the AES peak ratio Cl/Pd of a c(2×2)-Cl structure on Pd(100) surface (Θ_{VI} = 0.5 ML)). It is of interest that the interatomic distances of the Cl adlayer on Pd(110) for s1 structure are 3.3 and 3.89 Å, while the Cl–Cl distance of s2 is 3.86 Å, corresponding to the value obtained from Cl adlayer on Cu(111) under UHV conditions [25] which is slightly larger than 3.7 Å found for the Cl adlayer on the Cu/Pt(111) surface [9], obviously caused by the surface morphology. In contrast to Pd(110), no superstructure due to Cl adsorbate was observed from Pt(110) electrode surfaces.

4. Summary

The cyclic voltammogram of Cu UPD on Pd(110) demonstrates that complete Cu coverage is formed by two energetically well-separated steps, each associated with one monolayer Cu deposition which is identical to Cu UPD onto Pt(110) surface. However, in the presence of chloride ions, a pronounced change in the voltammogram for Cu UPD on Pd(110) was observed. The well-separated voltammetric peaks as found for the Cl^--free solution are transformed to several broad peaks. It was clearly caused by the specific adsorption of chloride anions as proven by the formation of ordered Cl adlayers (s1 and s2). On Pt(110) only slight change in voltammetric features was found, indicating no specific adsorption of Cl^- ions on Cu/Pt(110) as demonstrated by the diffraction patterns and the AES measurements for Cl adsorbate [16].

Acknowledgements

I wish to thank Prof. G. Ertl, Prof. D. M. Kolb and Dr. G. Lehmpfuhl for helpful discussions and for a critical review of the manuscript.

References

1. J. W. Schultze and D. Dickertmann, Surf. Sci. **54** (1976) 489.
2. E. Schmidt, P. Beutler and W. J. Lorenz, Ber. Bunsenges. Phys. Chem. **75** (1971) 71.
3. Y. Nakai, M. S. Zei, D. M. Kolb and G. Lehmpfuhl, Ber. Bunsenges. Phys. Chem. **88** (1984) 340.

4. M. S. Zei, G. Qiao, G. Lehmpfuhl and D. M. Kolb, Ber. Bunsenges. Phys. Chem. **91** (1987) 349.
5. D. M. Kolb, K. Al Jaaf-Golze and M. S. Zei, *DECHEMA-Monographien Bd. 102*, VCH Weinheim (1986) p. 53.
   D. M. Kolb, Z. Phys. Chem. N.F. **154** (1987) 179.
   T. Hachiya, H. Honbu and K. Itaya, J. Electroanal. Chem. **315** (1991) 275.
   Z. Shi and J. Lipkowski, J. Electroanal. Chem. **365** (1994) 303.
6. O. M. Magnussen, J. Hotlos, R. J. Nichols, D. M. Kolb and R. J. Behm, Phys. Rev. Lett. **64** (1990) 2929.
7. O. M. Magnussen, J. Hotlos, G. Beitel, D. M. Kolb and R. J. Behm, J. Vac. Sci. Technol. B **9** (1991) 969.
   T. Hachiya, H. Honbo and K. Itaya, J. Electroanal. Chem. **315** (1991) 275.
8. O. R. Melroy, M. G. Samant, G. L. Borges, J. G. Gordon, L. Blum, J. H. White, M. J. Albarelli, M. McMillan and H. D. Abruna, Langmuir **4** (1988) 728.
   M. F. Toney, J. H. Howard, J. Richter, G. L. Borges, J. G. Gordon, O. R. Melroy, D. Yee and L. B. Sorensen, Phys. Rev. Lett. **75** (1995) 4472.
9. R. Michaelis, M. S. Zei, R. S. Zhai and D. M. Kolb, J. Electroanal. Chem. **339** (1992) 299.
10. N. Markovic and P. N. Ross, Langmuir **9** (1993) 580.
11. N. Markovic, H. A. Gasteiger and P. N. Ross, Langmuir **11** (1995) 4098.
    I. M. Tidswell, C. A. Lucas, N. M. Markovic and P. N. Ross, Phys. Rev. B **51** (1995) 10205.
12. H. S. Yee and H. D. Abruna, Langmuir **9** (1993) 2460.
    R. Gomez, H. Y. Yee, G. M. Bommarito, J. M. Feliu and H. D. Abruna. Surf. Sci. **335** (1995) 101.
13. H. Matsumoto, J. Inukai and M. Ito, J. Electroanal. Chem. **379** (1994) 223.
    K. Sashikata, N. Furuya and K. Itaya, J. Electroanal. Chem. **316** (1991) 361.
14. R. Michaelis and D. M. Kolb, J. Electroanal. Chem. **328** (1992) 341.
15. D. Aberdam, R. Durand, R. Faure and F. El-Omar. Surf. Sci. **162** (1985) 782.
16. M. S. Zei and G. Ertl, Z. Phys. Chem. **202** (1997) 5.
17. D. M. Kolb, G. Lehmpfuhl and M. S. Zei, *NATO-ASI Series C. Spectroscopic and Diffraction Techniques in Interfacial Electrochemistry.* Kluwer Acad. Publishers (1990).
18. R. L. Gerlach and T. N. Rhodin, Surf. Sci. **17** (1969) 32.
19. R. Michaelis and D. M. Kolb, Surf. Sci. **234** (1990) L281.
20. R. Michaelis, Ph. D. Thesis, Free University Berlin (1991).
21. J. E. Houston and R. L. Park, Surf. Sci. **21** (1970) 209.
22. W. Berndt, Surf. Sci. **219** (1989) 161.
23. J. F. Wendelken, G. C. Wang, J. M. Pimbley and T. M. Lu, Mat. Res. Soc. Symp. Proc. Vol. **41** (1985) 171.
24. T. M. Lu, G. C. Wang and M. G. Lagally, Surf. Sci. **107** (1981) 494.
25. P. J. Goddard and R. M. Lambert, Surf. Sci. **67** (1977) 180.